Ablation of Porcine Ligamentum Flavum with Ho:YAG, Q-Switched Ho:YAG, and Quadrupled Nd:YAG Lasers

Matt R. Johnson, BS,[1] Patrick J. Codd, MD,[2] Westin M. Hill, BS,[1] Tara Boettcher, BS[1]
[1]Massachusetts Institute of Technology, Lincoln Laboratory, 244 Wood Street, Lexington, MA 02420
[2]Massachusetts General Hospital, Harvard Medical School, Department of Neurosurgery, 55 Fruit Street, Gray 502, Boston, MA 02114

ABSTRACT

Background and Objectives: Ligamentum flavum (LF) is a tough, rubbery connective tissue providing a portion of the ligamentous stability to the spinal column, and in its hypertrophied state forms a significant compressive pathology in degenerative spinal stenosis. The interaction of lasers and this biological tissue have not been thoroughly studied. Technological advances improving endoscopic surgical access to the spinal canal makes selective removal of LF using small, flexible tools such as laser-coupled fiber optics increasingly attractive for treatment of debilitating spinal stenosis. Testing was performed to assess the effect of Ho:YAG, Q-switched Ho:YAG, and frequency quadrupled Nd:YAG lasers on samples of porcine LF. The objective was to evaluate the suitability of these lasers for surgical removal of LF.

Study Design/Materials and Methods:
Ligamentum flavum (LF) was resected from porcine spine within two hours of sacrifice and stored in saline until immediately prior to laser irradiation, which occurred within an additional two hours. The optical absorbance of the samples was measured over the spectral band from 190 to 2360 nm both before and after dehydration. For the experiments using the Ho:YAG (λ = 2080 nm, t_p = 140 µs, FWHM) and Q-Switched Ho:YAG (λ = 2080 nm, t_p = 260 ns, FWHM) lasers, energy was delivered to the LF through a laser-fiber optic with 600 µm core and NA = 0.39. For the experiment using the frequency quadrupled Nd:YAG laser (λ = 266 nm, t_p = 5 ns FWHM), the energy was focused through a series of lenses onto the LF. Five experiments were conducted to evaluate the effect of the given lasers on LF. First, using the Ho:YAG laser, the single-pulse laser-hole depth vs. laser fluence was measured with the laser-fiber in direct contact with the LF (1 gram force) and with a standoff distance of 1 mm between the laser-fiber face and the LF. Second, with the LF remaining *in situ* and the spine bisected along the coronal plane, the surface temperature of the LF was measured with an IR camera during irradiation with the Ho:YAG laser, with and without constant saline flush. Third, the mass loss was measured over the course of 450 Ho:YAG pulses. Fourth, hole depth and temperature were measured over 30 pulses of fixed fluence from the Ho:YAG and Q-Switched Ho:YAG lasers. Fifth, the ablation rate and surface temperature were measured as a function of fluence from the Nd:YAG laser. Several LF staining and hole-depth measurement techniques were also explored.

Results:
Aside from the expected absorbance peaks corresponding to the water in the LF, the most significant peaks in absorbance were located in the spectral band from 190 to 290 nm and persisted after the tissue was dehydrated. In the first experiment, using the Ho:YAG laser and with the laser-fiber in direct contact with the LF, the lowest single-pulse fluence for which LF was visibly removed was 35 J/cm^2. Testing was

conducted at 6 fluences between 35 J/cm^2 and 354 J/cm^2. Over this range the single-pulse hole depth was shown to be near linear (R^2 = 0.9374, M = 1.6), ranging from 40 µm to 639 µm (N=3). For the case where the laser-fiber face was displaced 1 mm from the LF surface, the lowest single-pulse fluence for which tissue was visibly removed was 72 J/cm^2. Testing was conducted at 4 energy densities between 72 J/cm^2 and 180 J/cm^2. Over this range the single-pulse hole depth was shown to be nearly linear (R^2 = 0.8951, M = 1.4), ranging from 31 µm to 220 µm (N=3). In the second experiment, with LF *in situ*, constant flushing with room temperature saline was shown to drastically reduce surface temperature during exposure to Ho:YAG at 5 Hz with the laser-fiber in direct contact with the LF. Without saline, over one minute of treatment with a per-pulse fluence of 141 mJ/cm^2, the average maximum surface temperature measured 110 °C. With 10 cc's of saline flushed over one minute and a per-pulse laser fluence of 212 mJ/cm^2, the average maximum surface temperature was 35 °C. In the third experiment, mass loss was found to scale linearly with delivered fluence over 450 pulses of 600 mJ (212 J/cm^2, direct contact, N = 4; 108 J/cm^2, 1 mm standoff, N = 4) from the Ho:YAG laser. With the laser-fiber in direct contact, an average of 53 mg was removed (R^2 = 0.996, M = 0.117) and with 1 mm laser-fiber standoff, an average of 44 mg was removed (R^2 = 0.9988, M = 0.097). In the fourth experiment, 30 pulses of the Ho:YAG and Q-Switched Ho:YAG lasers at 1 mm standoff and 5 Hz produced similar hole depths for the tested fluences of 9 J/cm^2 (151 µm and 154 µm, respectively) and 18 J/cm^2 (470 µm and 442 µm, respectively), though the Ho:YAG laser produced significantly more carbonization around the rim of the laser-hole. The increased carbonization was corroborated by higher measured LF temperature. In all tests with the Ho:YAG and Q-Switched Ho:YAG, an audible photo-acoustic affect coincided with the laser pulse. In the fifth experiment, with the frequency quadrupled Nd:YAG laser at 15 Hz for 450 pulses, ablation depth per pulse was shown to be linear for the fluence range of 0.18 J/cm^2 to 0.73 J/cm^2 (R^2 = 0.989, M = 2.4). There was no noticeable photo-acoustic effect nor charring around the rim of the laser-hole.

Conclusion:

The Ho:YAG, Q-Switched Ho:YAG, and frequency quadrupled Nd:YAG lasers were shown to effectively remove ligamentum flavum (LF). A single pulse of the Ho:YAG laser was shown to cause tearing of the tissue and a large zone of necrosis surrounding the laser-hole. Multiple pulses of the Ho:YAG and Q-Switched Ho:YAG lasers caused charring around the rim of the laser-hole, though the extent of charring was more extensive with the Ho:YAG laser. Charring caused by the Ho:YAG laser was shown to be mitigated by continuously flushing the affected LF with saline during irradiation. The Nd:YAG laser was demonstrated to ablate LF with no gross visible indication of thermal damage to surrounding LF.

Key words: lumbar spinal stenosis; LSS; laminectomy; nerve pain; spinal canal.

INTRODUCTION

Lumbar spinal stenosis (LSS) is a condition where a narrowing of the spinal canal causes the compression of important neural structures such as the spinal cord and nerve roots. The result is a spectrum of disorders that can include painful shock-like sensations, pain in the extremities, and the potential loss of motor and sensory function. It is estimated that LSS affects 1.2 million people in the United States and constitutes a significant detriment to the quality of life for an aging population [1,2]. Although chronic intervertebral disc degeneration and bony hypertrophy can both contribute to the narrowing of the spinal canal, the fundamental offending pathology in the majority of LSS patients is the thickening of the collagenous connective tissue bridging the interlaminar spaces of the dorsal spinal canal called the ligamentum flavum (LF). Thickening of the LF can account for as much as 85% of lumbar spinal canal narrowing in degenerative cases of LSS [3]. Fortunately, flexion/extension studies have

shown that an approximate 16% increase in canal diameter could be sufficient to significantly relieve the pain and disability caused by symptomatic LSS [4]. The surgical challenge then becomes access and removal of the problematic LF.

Contemporary surgical treatments for LSS centers about surgical removal of compressive bony overgrowths and thickened ligamentum flavum via a procedure involving dissecting away the surrounding back muscles, drilling away bone, and manually removing thickened tissue using rongeurs and tissue punch instrumentation. In 2006, approximately 162,000 such decompressive laminectomies were performed by neurosurgeons for LSS in the United States alone [5]. Though the laminectomy provides an effective means by which to relieve LSS by removing the offending bony and soft tissue overgrowths, it comes at the surgical cost of general anesthesia, extensive bone removal and collateral tissue dissection and damage, prolonged postoperative recovery times extending for weeks or months, and the need for extensive physical therapy and medicinal pain management.

Attempts to mitigate the collateral soft tissue destruction and morbidity associated with classic laminectomy techniques for removing hypertrophied LF have recently explored minimally invasive access to the spinal canal. These have included the use of interlaminar spacers to open the intervertebral space, minimally invasive laminotomies via tubular retractor systems and endoscopic visualization, as well as wider laminectomies with placement of pedicle screw/rod hardware. As surgical access to the spinal canal is achieved through narrower corridors, endoscopic approaches to LSS treatment become more appealing. Endoscopes employing digital visualization technology and tools for precise pathology targeting with fiber-coupled lasers have the potential to facilitate the surgical procedure with minimal collateral tissue disruption, thereby minimizing patient discomfort and reducing recovery times.

Fiber-coupled laser removal of LF may provide a method to decompress the spinal canal while avoiding the adverse side effects of the current surgical approach. Therefore, it is useful to investigate the suitability of lasers to remove LF. Here we investigate the impact of Ho:YAG and Nd:YAG lasers on samples of porcine LF and characterize the interaction effects with the goal of tissue ablation.

MATERIALS AND METHODS

Excision of ligamentum flavum (LF)

All porcine spines were obtained from a local slaughterhouse within 2 hours post-mortem. All procedures were conducted in accordance with protocols approved by the Massachusetts Institute of Technology Committee on Animal Care (E13-09-0516).

Porcine spines were dissected along the coronal plane, splitting the mid body of the pedicle to separate the dorsal from the ventral components of the vertebral column, exposing the dorsal surface of the spinal canal and the associated LF segments bridging each vertebral level. LF was subsequently excised from its superior and inferior ventral laminar surface attachments and transferred into Phosphate-buffered Saline (PBS) at room temperature until used for laser experiments, occurring within 2 hours of harvest.

Optical absorbance of ligamentum flavum (LF)

Immediately after excision from porcine spine the LF was placed between two pure fused silica plates (1.0” diameter, 1/16” thick; Bond Optics, LLC) which were secured in a 25 mm lens tube (Thorlabs, Inc.). The transmission and reflection of the samples were measured from a wavelength of 190 nm to 2360 nm in 1 nm steps using a Spectrometer (PerkinElmer Lambda1050) and integrating sphere, both within 20 minutes of removal (wet sample) and after three days of storage in a desiccated container (dry sample, <3% humidity). Absorbance was calculated after subtracting the baseline

measurement taken with no LF sample between fused silica plates in order to account for variance in fused silica transmission/reflection, light source output, and receiver sensitivity as a function of wavelength. The baseline, transmission, and reflection measurements were used to calculate the optical absorbance of LF as a function of wavelength.

Ho:YAG laser source characterization

A TM2000 Ho:YAG laser (Equilasers, Model EHL-20) was modified such that its output energy could be measured during operation using a beam-sampler and power meters (Ophir PE-25C). An acousto-optic Q-Switch (Gooch & Housego, LLC; MQS027-4S20V6-8-200PP), driven by a 200W RF driver (Gooch & Housego, LLC, A23027-A-5/600-S4K7U) was also added. In addition, the power supply of the TM2000 was modified such that the pulse-to-pulse variability was minimized, thereby producing consistent pulse energies (~4 mJ standard deviation over 30 pulses). In order to verify the expected output energy, the pulse energy was measured at the output of the low-power beam sample as well as the output of the laser-fiber (600 µm core diameter, Thorlabs, M29L01, NA = 0.39) for 30 laser firings prior to each test. For each set of 30 firings, a coefficient was determined that accurately related the power recorded from the low-power beam sample measurement to that at the laser-fiber tip. The pulse width of the laser was measured with an InGaAs detector (Thorlabs, PDA-10D, 15 MHz bandwidth) and oscilloscope (Tektronix, MSO4104B, 1 GHz bandwidth). The pulse width was measured to be 140 µs (FWHM, un-Q-switched) or 260 ns (FWHM, Q-switched). The laser output energy was experimentally determined to reach a consistent level after ten pulses, so the laser was fired 10 times with its mechanical output shutter closed before the shutter was opened and the tissue irradiated.

Ho:YAG laser-fiber beam quality

In order to characterize the spatial uniformity of the Ho:YAG irradiation, the beam at the laser-fiber face was magnified (8.3x, 4-f optical system) and imaged onto a pyroelectric solid-state camera (Ophir, Pyrocam III). As illustrated in *figure* 1, the beam was shown to have an approximate top-hat profile. The plateau uniformity, $U_P(z)$, was measured to be 0.002, where:

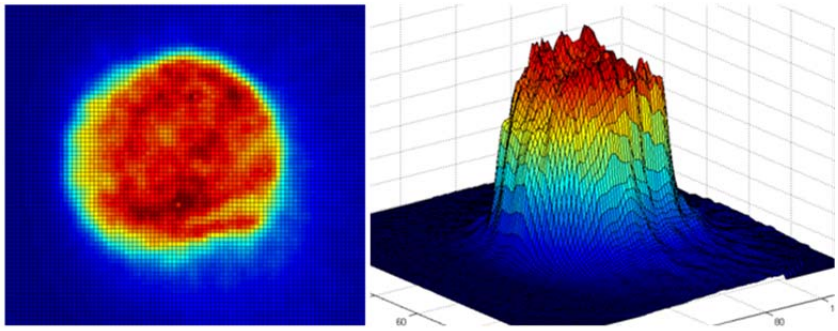

Figure 1: Two-dimensional (A) and three-dimensional (B) images of Ho:YAG 600 µm core laser-fiber face. Spatial output profile shown to be near top hat.

$$U_P(z) = \frac{\Delta E_{FWHM}}{E_{max}} \ ;$$

ΔE_{FWHM} is the full-width at half-maximum of the peak near E_{max} of the power/energy density histogram [6].

The edge steepness, s(z), which is defined as the normalized difference between effective irradiation areas of 10% ($A^i_{0.1}$) and 90% ($A^i_{0.9}$) of peak with power/energy density values of 10% of peak, was measured to be 0.922), where [6]:

$$s(z) = \frac{A^i_{0.1}(z) - A^i_{0.9}(z)}{A^i_{0.1}(z)}$$

Ho:YAG laser-fiber direct contact and 1 mm standoff to ligamentum flavum (LF)

For tests where the laser-fiber was in direct contact with the tissue, the LF was placed on a custom stage, which allowed the LF to be tilted such that the flat LF surface was parallel to the laser-fiber face. The pivoting stage was placed on a scale (Sartorius, TE2145) and the laser-fiber was secured to a moveable optical stage, allowing for very fine mechanical control of the laser-fiber relative to the LF. The optical stage was used to move the laser-fiber into direct contact with the LF until the scale measured 1 gram, at which point the laser was fired. In the case where the laser was fired at a standoff of 1 mm from the laser-fiber face to the LF surface, the laser-fiber was advanced toward the LF until any positive mass registered on the scale, and then retreated by 1 mm, as measured by the optical stage. For cases where the laser-fiber was in direct contact with the LF, given that the beam exiting the laser-fiber was not diffraction limited and based on the measured plateau uniformity and edge steepness, the fluence is taken to be the total output energy divided by the total area of the 600 µm laser-fiber core. For cases where the laser-fiber is 1 mm removed from the LF, the fluence was adjusted for the reduced energy density based on the laser-fiber's numerical aperture of 0.39 as specified by the vendor.

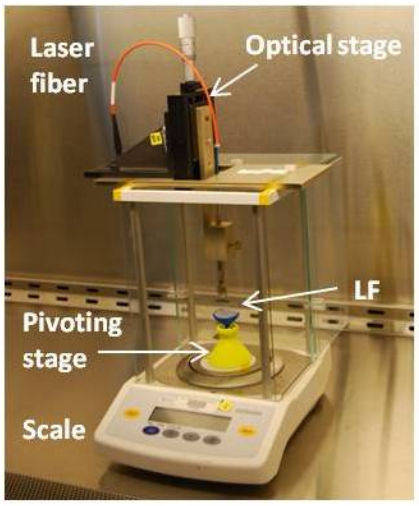

Figure 2: Laser fiber and LF holding fixture on scale.

Mass loss of ligamentum flavum (LF) due to treatment with Ho:YAG laser

For measurement of mass loss of LF due to treatment with the Ho:YAG laser, the samples of LF were placed on a scale (Sartorius, TE2145) and the starting mass of the sample noted. The LF was treated with 30 shots of the Ho:YAG (600 mJ; 212 J/cm^2 [direct contact], 108 J/cm^2 [1 mm standoff]) via laser-fiber and the mass was again noted. This sequence was repeated until the sample had been treated with 450 laser pulses. N = 4 (direct laser-fiber contact) and N = 4 (1 mm laser-fiber standoff).

Nd:YAG laser source characterization

A frequency quadrupled Q-switched Nd:YAG (λ = 266 nm, FWHM = 5 ns; Continuum MiniLite) was focused to an almond shaped spot with dimensions 542 x 868 µm, as measured by a reticle-equipped microscope view of ablated photoresist. Output power was measured directly with a power meter (Ophir PE-25C) before and after testing and found to be unchanged within the resolution of the meter. The sample of LF was placed within the Rayleigh region of the laser spot and irradiated for 450 pulses. The ablation rate was calculated by dividing the laser-hole depth by the number of pulses. The beam was not profiled and very likely contained hot spots.

Measurement of laser-hole depth in ligamentum flavum (LF)

Immediately after the LF was treated with the laser, the laser-hole dimensions were measured using an optical microscope at 63x magnification (Olympus, SZX12; 6.3x eyepiece lens, objective lens B Plan Apo, 10x/0.28, f=200, ∞/0) with integrated displacement meter (Boeckeler 302M) and digital

readout (Quadra-Chek 200). The length and width were measured by lining up the edge of the laser-hole with the cross-hair built into the microscope lens, zeroing the displacement stage, panning to the opposite side of the laser-hole, and recording the lateral displacement of the specimen stage. The laser-hole depth was measured using the narrow depth of focus (DOF) technique. Taking the average visible wavelength (λ) to be 545 nm and the numerical aperture (NA) of the lens to be 0.28, the quarter-wave DOF can be approximated as

$$DOF = +/-[\frac{\lambda}{2 * NA^2}]$$

giving a DOF of +/- 3.5 µm. For the narrow depth of field technique, the operator optically focused on the bottom of the laser-hole, zeroed out the displacement readout, and lowered the specimen stage until the rim of the laser-hole came into optical focus. The distance the specimen stage traveled between focus at the bottom of the laser-hole and the top of the laser-hole was taken to be the laser-hole depth.

Ligamentum flavum (LF) sectioning and staining

In order to view the tissue pathology two sample preparation techniques were employed. After the LF was treated with the laser, the laser-hole was cut in half with a razor blade. Half of the tissue was fixed in 10% formalin overnight, then moved to and oriented in histology cassettes in 70% ethanol. Samples were paraffin embedded and sectioned (10µm) perpendicular to the laser incision. Sections were subsequently stained with hematoxylin and eosin (H&E). Measurements of depth, width and the extent of thermal damage were made using a light microscope. Zones of carbonization, cellular vacuolization, and coagulation were noted.

For the second technique, employed as an alternate method of viewing the live/dead boundary in the laser-affected area, the remaining half of the laser-hole was incubated in calcein AM (1.6µM) and ethidium homodimer-1 (0.8µM or 1.6µM) for 2 hours at room temperature (Live/Dead viability/cytotoxicity kit for mammalian cells, Molecular Probes), washed with PBS, and analyzed by confocal microscopy (Nikon), similar to Mainil-Varlet [7]. Living cells yield a green fluorescent product (calcein) by the enzymatic conversion of the virtually non-fluorescent cell-permeant calcein AM to calcein, using the presence of ubiquitous intracellular esterase activity. Ethidium homodimer-1 is a red fluorescent nucleic acid stain that is able to pass through damaged plasma membranes of injured or dead cells, and is excluded by the intact plasma membrane of live cells. Measurements of depth, width, and the extent of thermal damage were made.

Thermal measurements

During laser irradiation the thermal response of the treated surface was measured and recorded with an IR camera (FLIR A600 Series; lens f=13.1, P/N T197526) at 22 fps. Although the camera frame rate is slow relative to the laser pulsewidth and therefore not useful for measuring peak temperature, it is useful in generally characterizing tissue temperature in the region. Raw pixel data was recorded from the camera onto a computer. For the purpose of translating pixel counts to temperature, the tissue was assumed to have the same emissivity as human skin, 0.98, which is the same as water [8]. The maximum measureable temperature of the IR camera is 160 °C. In order to accurately mimic *in situ* thermal boundary conditions, LF was left in a bisected porcine spine and the Ho:YAG laser was applied at 5 Hz for 60 seconds through a 600 µm-core laser-fiber, which was in direct contact with the tissue during irradiation. The surface temperature was measured both without constant flushing with saline and with constant flushing at a rate of 10 cc over one minute. The laser-fiber was contained within a polyimide tube through which saline could flow around the laser-fiber and directly onto the irradiated area.

RESULTS

Optical absorbance of ligamentum flavum (LF)

Figure 3 shows the absorbance of LF vs. wavelength from 190 nm – 2360 nm. In addition to the absorption peaks associated with water in the LF near 1.5 µm and 1.9 µm [9], there exist absorption peaks between 190 nm – 290nm. The absorption peaks not associated with the water persist after the tissue is dried, whereas the absorption peaks associated with the water in the LF are largely reduced.

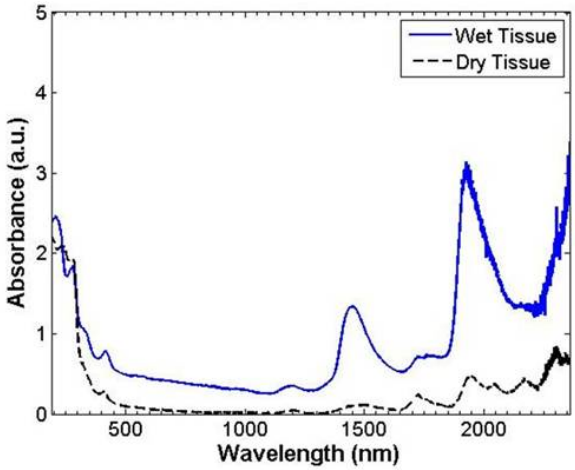

Figure 3: Absorbance of LF as a function of wavelength when freshly excised and after dehydration.

Ho:YAG - Hole depth for direct laser-fiber contact vs. 1 mm laser-fiber standoff

Figure 4 shows the single-pulse hole-depth caused by the Ho:YAG laser with the laser-fiber in direct contact with the tissue as well as at a distance of 1 mm (N = 3 for each condition). Laser-hole depth vs. fluence was very near linear for both the direct laser-fiber contact and 1 mm standoff conditions. The laser-holes in the LF were not circular, but approximately of an ovular shape. For the direct laser-fiber contact test condition, the average length-to-width ratio of the laser-hole was 1.3, with a standard deviation of 0.24, where the largest dimension was taken to be the length. The maximum laser-hole length was 829 µm, the minimum was 487 µm, and the average 613 µm (σ = 101 µm). For the 1 mm laser-fiber standoff test condition, the average length-to-width ratio was 2.2, with σ = 0.40, where the largest dimension of the laser-hole was taken to be the length. The maximum laser-hole length was 542 µm, the minimum was 263 µm, and the average 429 µm (σ = 94 µm). When measuring the laser-hole depth, both laser-holes created under direct laser-fiber contact as well as those with 1 mm standoff conditions appeared to be free of residual debris. However, when the LF was stained with H&E and sectioned, all samples that had been tested under the 1 mm

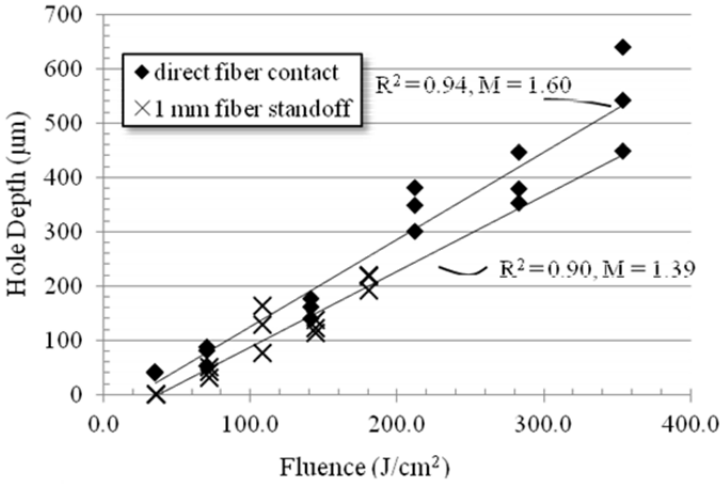

Figure 4: Laser-hole depth as a function of fluence for Ho:YAG laser with the laser-fiber in direct contact with the LF, and with 1 mm laser-fiber standoff.

laser-fiber standoff condition appeared to have been shredded rather than cleanly removed. This effect is shown in *figure 5*. When the LF was irradiated with the laser-fiber in direct contact, the LF sample rapidly jumped and impaled itself on the laser-fiber. In addition, *figure 6 shows* a frame taken from a MIT Lincoln Laboratory-developed IR camera with a frame-rate of 1000 fps; steam can be seen rapidly exiting the side of the LF during irradiation.

Figure 7 shows the two halves of the same laser-hole; one side was prepared with live/dead stain and the other with H&E. Macroscopic tearing and extensive cellular necrosis is evident adjacent to the laser-hole.

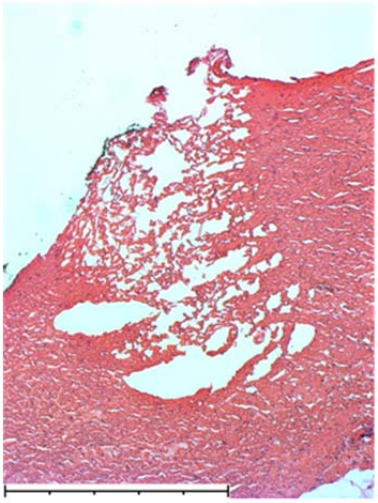

Figure 5: 10 µm thick section of LF stained with H&E. LF was treated with Ho:YAG laser with 1 mm laser-fiber standoff. Bar is 500 µm in length.

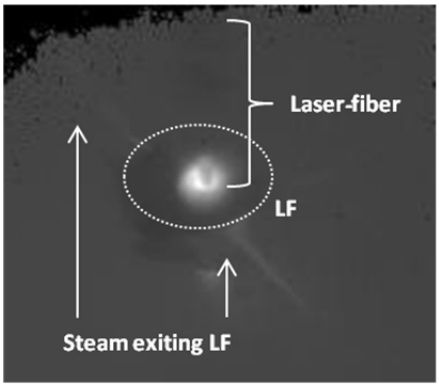

Figure 6: Frame from IR video captured at 1000 frames-per-second. Shows steam rapidly exiting sample during irradiation. Fiber was in direct contact with tissue and fluence = 212 mJ/cm^2.

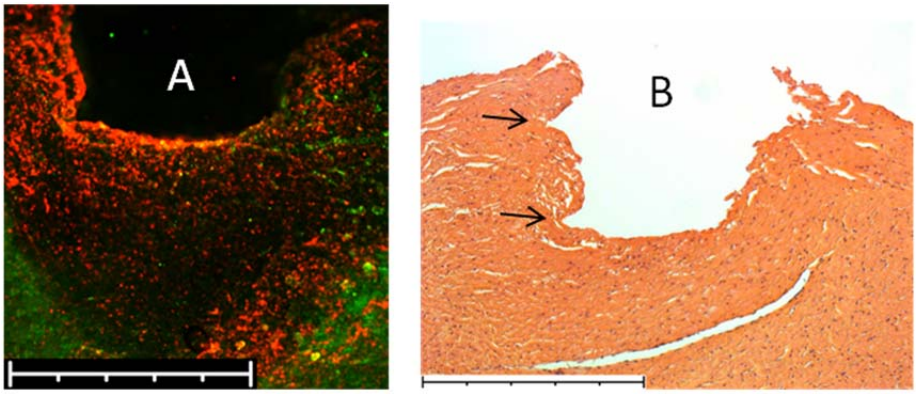

Figure 7: Laser-holes resulting from treatment with Hol:YAG laser with laser fiber in direct contact with the LF. (A) and (B) were treated with one pulse of 283 mJ/cm^2. A = live/dead stain; B = H&E stain. White and black bars are 500 µm. Black arrows point to torn LF.

Ho:YAG gross thermal response

With an applied per-pulse fluence of 141 mJ/cm^2 and no saline flush, the maximum average surface temperature was 110 °C (*figure 8a*) and the remaining LF was significantly charred (*figure 8c*). With an applied fluence of 212 mJ/cm^2, and constant flushing with room temperature saline (10 cc/min) the maximum average surface temperature was 35 °C (*figure 8b*) and the remaining LF was not charred (*figure 8d*).

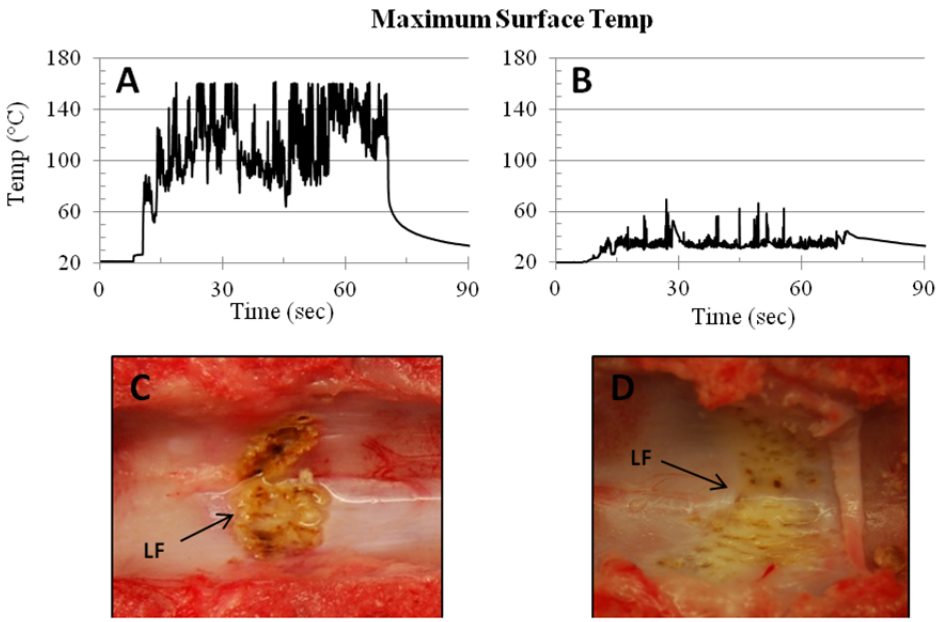

Figure 8: Maximum surface temperature resulting from 60 seconds of treatment with Hol:YAG laser at 5 Hz to LF *in situ* with and without saline flush. (A, C): No saline flush, 142 mJ/cm^2, average surface temp = 110 °C. (B, D): Continuous saline flush at 10 cc/min and 212 mJ/cm^2, average surface temp = 35 °C.

Ho:YAG - Mass loss over multiple laser shots

Figure 9 shows the mass loss over the course of 450 Ho:YAG laser pulses delivered with energy of 600 mJ with the laser-fiber both in direct contact (212 J/cm^2) as well as displaced 1 mm (108 J/cm^2), (N = 4 for each condition). In both cases the rate of mass loss was very near linear (direct contact R^2 = 0.996, 1 mm R^2 = 0.9988) though the slope was slightly less for the 1 mm laser-fiber standoff case. As shown in *figure 10*, the tissue was grossly charred at the completion of testing.

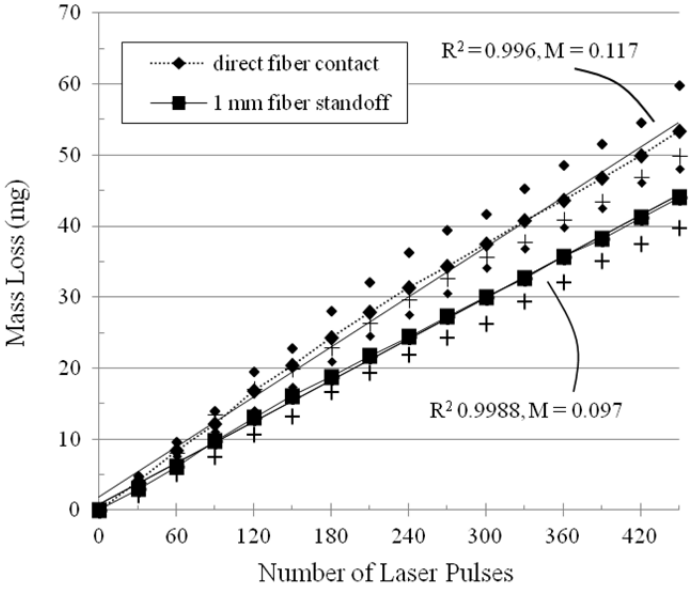

Figure 9: Average, maximum, and minimum mass loss of LF treated with Hol:YAG through 600 µm fiber, 5 Hz, 600 mJ.

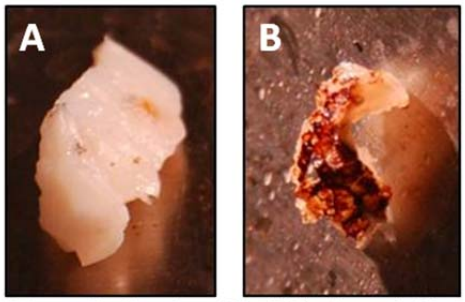

Figure 10: Samples of LF (A) before and (B) after mass loss test, which consisted of 450 pulses of 600 mJ. Level of charring appeared similar both when laser-fiber was in direct contact with tissue and stood off my 1 mm.

Ho:YAG – Hole depth and temperature for non-Q-Switched vs. Q-Switched

Figure 11 shows the laser-hole depth for the same Ho:YAG pulse energies applied without the Q-Switch active (t_p = 140 µs, FWHM) and with the Q-Switch active (t_p = 260 ns, FWHM). Tests were conducted at per-pulse fluences of 4.5 J/cm^2, 9 J/cm^2, and 18 J/cm^2 with 1 mm standoff between the laser-fiber face and the LF for 30 pulses at a rate of 5 Hz (N = 3 for each condition). With a per-pulse fluence of 4.5 J/cm^2, only surface dehydration or charring was visible. For all tested laser modes and energies, the laser-hole depth was very comparable. However, as shown in *figure 12*, carbonization was more pronounced without the Q-Switch active. Moreover, it was observed that the entire sample of LF constricted as the 30 laser pulses were delivered, resulting in the LF sample curling up in the direction of the laser-hole.

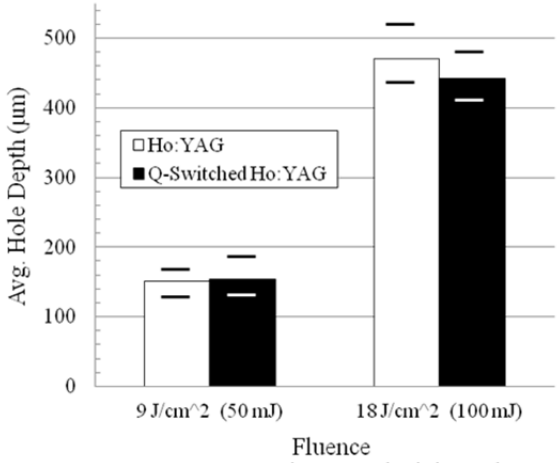

Figure 11: Average, maximum, and minimum laser-hole depth in LF after 30 pulses from Ho:YAG and Q-switched Ho:YAG laser.

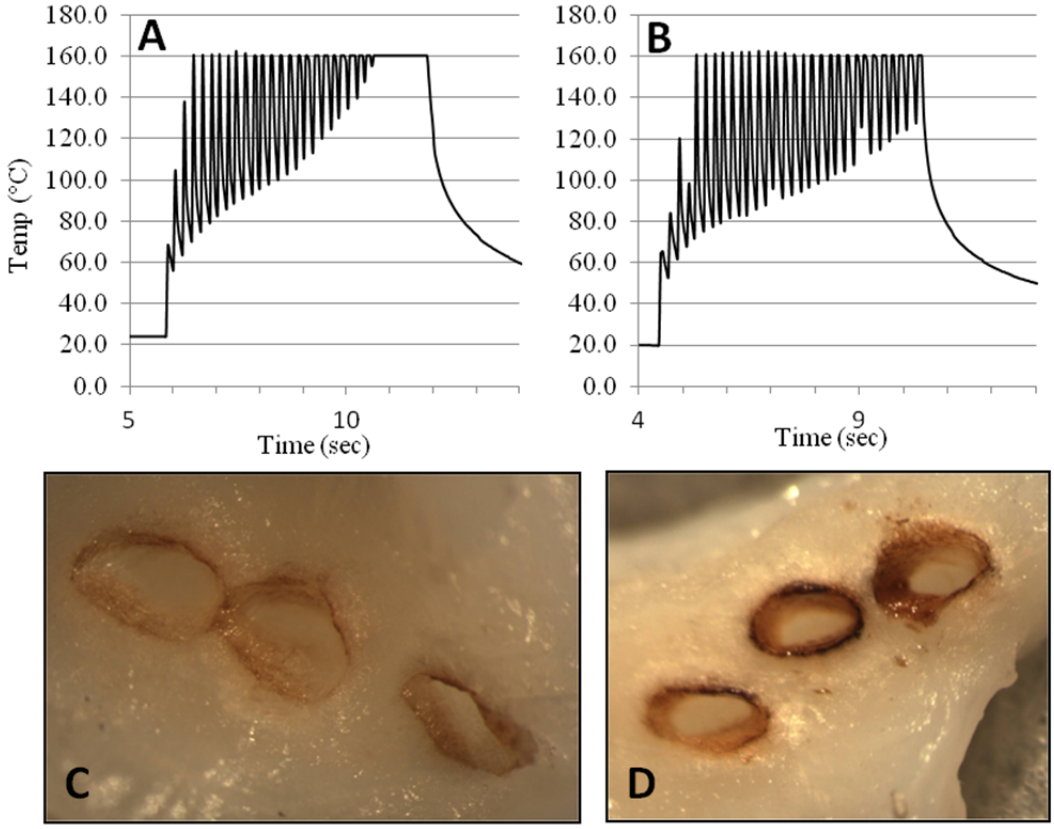

Figure 12: Measured surface temperature of a given test of LF treated with 30 pulses of Ho:YAG and Q-switched Ho:YAG at fluence 18 J/cm^2, 5 Hz rate with 1 mm laser-fiber standoff. (A and C, respectively). Photographs of laser-holes showing carbonization around the rim of the laser-holes for the Ho:YAG and Q-switched Ho:YAG lasers (C and D, respectively).

Nd:YAG – Ablation rate and temperature

As shown in figure 13, beyond the experimentally determined appreciable ablation threshold of the quadrupled Nd:YAG laser (0.176 J/cm^2), the ablation rate/pulse was shown to be very near linear (R^2 = 0.989, M = 2.4) up to 0.731 J/cm^2, where the employed laser reached its maximum output energy. The ablation rate remained unchanged by reducing the laser repetition rate from 15 Hz to 5 Hz. The reduction in repetition rate did however reduce the

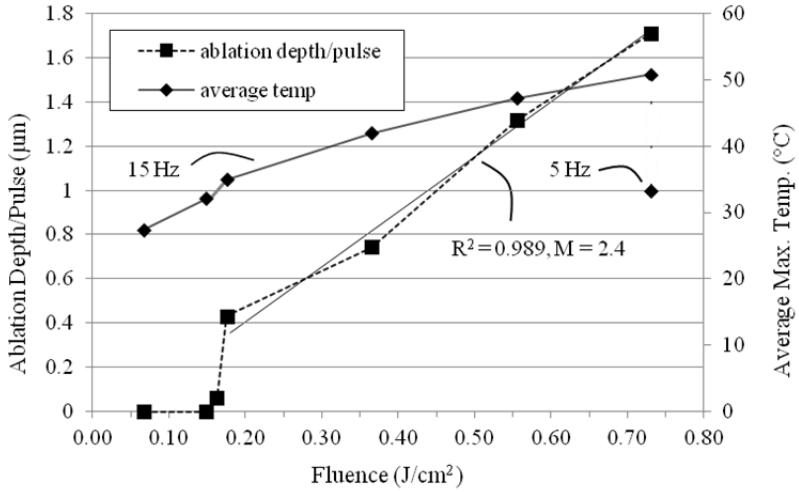

Figure 13: Measured maximum average surface temperature and ablation rate of LF with frequency quadrupled Nd:YAG laser.

maximum average temperature from 51 °C to 33 °C. No photoacoustic effect or curling of the LF was observed and, as shown in figure 14, there was no charring around the laser-hole.

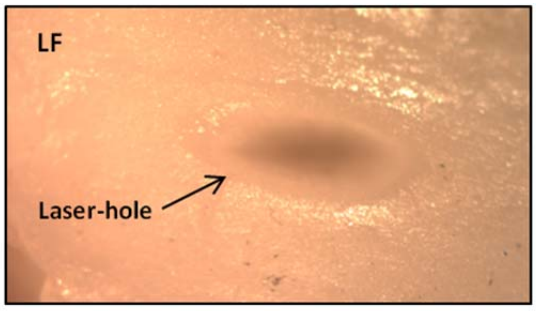

Figure 14: Laser-hole made in LF with frequency quadrupled Nd:YAG laser operating with a fluence of 0.731 mJ/cm^2 at a rate of 15 Hz. Laser-hole dimensions matched that of the irradiation pattern (~542 x 868 µm). No carbonization was visible.

DISCUSSION

Lumbar spinal stenosis (LSS) is a debilitating condition whose compressive pathology can lead patients to develop severe extremity pain, numbness, and even paralysis. A significant component of this condition results from compression of nerve roots and spinal cord through progressive overgrowth of the ligamentum flavum (LF), the connective tissue bridging adjacent vertebral levels within the spinal canal. MRI studies have suggested that as much as 85% of spinal canal narrowing is caused by hypertrophy of the ligamentum flavum [54]. This progressive degenerative condition affects a significant proportion of the aging population, with an estimated prevalence of symptomatic LSS at 8.4% affecting around 1.2 million people in the U.S. alone [10]. In 2006, approximately 162,008 open surgical decompressive laminectomies were performed by neurosurgeons in the U.S. in order to treat this condition [5]. This procedure requires extensive soft tissue dissection, spinal bone removal and mechanical removal of the offending tissue resulting in extended patient recovery times, rehabilitation needs, and patient discomfort. However, e*x vivo* spine mechanical studies suggesting that removal of as little as 16% of this thickened tissue could relieve LSS symptoms [4]. To this end, minimally invasive methods to selectively remove compressive LF stand to successfully strike at the offending pathology, thereby improving the quality of life for patients afflicted with this common condition.

Laser therapy has been used successfully to treat bulging or herniated intervertebral disc disease resulting in symptomatic spinal canal compression [11, 12] and the interaction of laser energy with intervertebral discs evaluated for common surgical lasers [13, 14]. However, utilization of lasers to specifically ablate hypertrophied ligamentum flavum as seen in degenerative LSS has not yet been explored. Here, we present a characterization of laser/LF interactions using three types of lasers: the Ho:YAG (λ = 2080 nm, t_p = 140 µs FWHM), the Q-Switched Ho:YAG (λ = 2080 nm, t_p = 260 ns FWHM), and the Q-Switched frequency quadrupled Nd:YAG (λ = 266 nm, t_p = 5 ns FWHM). The bulk absorption was measured as a function of wavelength and five experiments were conducted using the selected lasers.

The Ho:YAG laser (absorbance in fresh LF = 1.52 a.u.) was selected because it is a commonly deployed, fiber-coupled, surgical laser which is suitable for cutting many types of tissue due to its spectral proximity to the water absorption peak near 1.9 µm [15]. The Q-Switched Ho:YAG was selected to investigate the effect of laser pulsewidth on thermal injury to adjacent tissue. Although UV lasers are typically restricted to applications not requiring coupling to a flexible fiber optic, the Nd:YAG laser (λ = 266 nm, absorbance in LF = 1.78 a.u.) was selected because recent advances in High -OH fiber optics may enable the use of UV lasers for endoscopic applications [16]. In addition, for the effective laser removal of tissue, not only is the absorption of the chromophore of importance, but so too is the role of

the selected chromophore in the structure of the tissue [17]. Therefore, if water is the targeted chromophore, the water must be excited such that it strains and fractures the tissue comprising the extra cellular matrix (ECM). If the ECM is sufficiently robust, this will likely result in gross mechanical damage to surrounding tissue. If the targeted chromophore is that which comprises the ECM, the targeted tissue will be ablated with relatively reduced collateral mechanical or thermal damage. The bulk absorption, measured before and after dehydrating the LF, reveals absorption peaks near where they would be expected for water (1.44 μm, 1.95 μm), as well as where high absorption would be expected for protein, which contains a peptide bond (O=C-N-H) with absorption peak near λ = 190 nm [18]. Because LF is made up of elastic fibers and the protein collagen, high absorption in the UV is expected [19]. Therefore, although UV lasers are not currently used for endoscopic surgery, the potential benefits of directly targeting the ECM merit further investigation relative to ablation of LF.

The first experiment demonstrated that, over the tested fluence range, laser-hole depth increases linearly with fluence, regardless of the laser-fiber being in direct contact or displaced 1 mm from the LF. In addition, after adjusting the laser fluence for the increase in effected area due to the 1 mm laser-fiber displacement, the change in affect is minimal. The audible photo-acoustic effect, macroscopic tearing (*figure 7),* impaling of the LF onto the laser-fiber, and jets of steam (*figure 6*), indicate the removal process is subsurface explosion which results in the rapid ejection of material. This result is in agreement with previous studies using the pulsed Ho:YAG laser for removal of soft tissue [20]. The "shredding" affect shown in f*igure 5* is an example of the affect typically observed when the laser-fiber face was displaced by 1 mm from the LF surface. Initial inspection of the laser-hole through an optical microscope did not reveal the "shredded" tissue that appears in the laser-hole, but rather it appeared to be a clean blast site. It was only after the staining and sectioning process that that "shredded" tissue appeared in the laser-hole. This would indicate that the "shredded" tissue segments remain attached to the side-wall of the laser-hole, but are released during the staining and sectioning process, possibly when the LF is placed in liquids, including formalin and saline. In the case where the laser-fiber is in direct contact with the LF, however, the walls of the laser-hole appear cleanly cut, even after staining and sectioning (*figures 7B and 7D*). The difference may be due to the LF impaling itself on the laser-fiber when in direct contact with the LF, or due to the additional inertial confinement offered by the laser-fiber, resulting in more forceful ejection of material. Although macroscopic tearing and thermal damage may not be a notable risk when the adjacent tissue is LF, bone, or disc, it may be of concern when sensitive neural tissue such as the spinal cord is nearby. In the process of determining the best method for measuring hole depth (depth of field technique, live/dead, H&E), it was found that in order to achieve consistent measurements the depth had to be measured within minutes of the laser treatment, before the tissue dried out. Placing the LF in any liquid was found to cause swelling. Therefore, though the live/dead and H&E techniques were useful for viewing tissue histology, they were not reliable methods for quantifying laser-hole depth, zone of necrosis, or the magnitude of fissures.

The second experiment, which quantified the surface temperature with and without constant saline irrigation, demonstrated that irrigation can be an effective method to maintain reasonable surface temperatures and reduce carbonization. With regard to actual LF surface temperature between the two test conditions, though for the case where constant irrigation was applied the temperature of the saline was measured rather than the temperature of the LF surface, the measurements are still useful in giving a general sense of the thermal affect. As surgical tools are developed, it may prove useful to include the ability to continuously deliver saline directly to the laser-affected areas.

The third experiment showed that mass loss was linear for 450 laser pulses. The slope only slightly decreased for the case where the laser-fiber was displaced 1 mm from the LF surface compared to when the laser-fiber was in direct contact with the LF. Given that the Ho:YAG laser primarily targets water as the chromophore for tissue removal, it is not understood why the slope was linear over all 450 laser pulses. The expectation was that because the LF started the test in a well-hydrated state, and

therefore the water to be excited by the laser was abundant, the mass-loss per pulse efficiency would be much greater for the first several sets of pulses compared to the final pulses, where the LF demonstrated significant carbonization and had very little water left in it. This result could possibly be explained by the laser having an increased penetration depth in very dry versus well-hydrated tissue.

In the fourth experiment, as shown in *figure 12*, reducing the pulsewidth decreases thermal injury in the form of carbonization around the rim of the laser-hole without affecting the ablation rate. Given that the 600 µm core laser-fiber has a half-angle divergence of 23°, some of the carbonization may have been due to the reduced fluence around the edges of the laser-affected area.

The fifth experiment showed the ablation rate to be linear as a function of fluence using the frequency quadrupled Nd:YAG laser. This experiment was distinct from the experiments using the Ho:YAG lasers for several reasons. First, the wavelength targeted a chromophore other than water and therefore more likely directly targeted the Extra Cellular Matrix (ECM), resulting in direct cellular decomposition. Second, the pulsewidth was much shorter. Though the LF was not sectioned after being irradiated, and therefore it was not determined if adjacent LF was affected at the cellular level, the LF adjacent to the laser-hole was, under microscopic examination at 63x, indistinguishable from that outside of the laser-spot. Third, the laser energy was focused to a spot on the LF, meaning it was not diverging as it passed through the LF. Therefore, though the effect on the LF was favorable, the precise contribution of each factor has not been quantified.

Several factors may influence the accuracy of our laser/tissue interaction assessment when looking to relate to the *in vivo* pathologic state. Excision of the LF tissue from its interlaminar attachments within the spinal canal during tissue preparation results in a natural relaxation of this otherwise stretched tissue. While this may have altered interaction characteristics, anecdotally, tissue removal in these excised specimens was similar to that seen in the un-dissected specimens (*figure 11*). Likewise, the LF tissue harvested here was from juvenile pigs, and may not represent precisely the analogous degenerative, hypertrophied LF state achieved in the older human specimen. Histologic studies in humans have demonstrated that normal LF is comprised of approximately 80% elastic fibers and 20% collagen fibers [19], whereas hypertrophied pathologic LF shows an increased collagen composition resulting in thickening [21, 22]. How this degenerative alteration in the collagen/elastin ratio affects the laser-tissue interactions will need further evaluation, including use of human hypertrophied LF samples for laser interaction testing. Given the laser's generally effective ablation of connective tissue, which has a high concentration of collagen fiber, we suspect that this change in ratio will have minimal effect on tissue ablation efficacy. With these caveats however, these data do provide a useful first understanding of LF/laser interaction properties.

Future work could include testing to assess the efficacy of several laser-ablation approaches. First, further exploration involving several components of tissue removal via directly targeting the ECM with UV lasers would be extremely informative. The principle chromophore in the short UV range is the peptide bond (O=C-N-H), with its absorption peak near λ = 190 nm [18]. Given that 20% of LF is the protein collagen, an excimer laser (λ = 193 nm) may prove effective against LF, though transmitting it through currently available, highly flexible, fiber optics will likely be more challenging than at 266 nm. Since the 266 nm laser was shown to effectively ablate LF, though at a very slow pulse repetition rate, it would be informative to perform additional testing at higher pulse repetition rates, where the ablation rate would likely be increased. In addition, since peak power may be a key limiting factor for transmission through a fiber optic, it would be useful to determine the longest pulsewidth (and therefore lowest peak power) for which the desired ablation affects occur. In order for UV lasers to be useful in endoscopic applications, a survey of and testing with available laser-fibers is necessary. Second, though targeting water as the chromophore has the disadvantage of not directly dissociating the ECM, and therefore may result in more damage to adjacent tissue, it has the advantage of being easily transmitted through readily available low-loss fiber optics. Therefore, it would be useful to perform

testing with lasers such as the Thulium fiber laser (λ = 1940 nm) in order to assess the impact of higher absorbance by the water contained in the tissue. Third, short-pulse lasers, with pulsewidths on the order of nanoseconds, picoseconds, or femtoseconds could be used to explore ablation of LF by mechanisms such that thermal damage is minimized. Fourth, focusing optics could be incorporated onto the tip of the laser-fiber in order to limit beam divergence, therefore minimizing the area of the LF that is exposed to energy under the ablation threshold, resulting in cleaner removal of tissue.

Here, we have presented the effect of the Ho:YAG, Q-Switched Ho:YAG, and frequency quadrupled Nd:YAG lasers on ligamentum flavum (LF). All lasers tested were shown to be capable of removing LF. Macroscopic mechanical and thermal damage to LF adjacent to the laser-hole was evident with the Ho:YAG and Q-Switched Ho:YAG lasers. Charring was shown to be reduced by shortening the laser pulsewidth or by constant flushing with saline. The Nd:YAG laser was shown to ablate LF with no damage to adjacent tissue, as perceived under visual microscope examination at 63X magnification without sectioning or staining.

The surgical implications of these findings are significant. The ability to effectively and selectively eliminate the fundamental compressive pathology in LSS offers the possibility of avoiding the soft tissue destruction and associated morbidity associated with contemporary minimally invasive lumbar decompression. Navigating a laser-fiber-coupled system to the site of ligamentum flavum hypertrophy within the spinal canal is a fundamental design challenge for a laser-driven minimally-invasive system. However, advances in percutaneous endoscopic navigation of the spinal canal have already been demonstrated using flexible endoscopes introduced through a small opening in the base of the sacrum called the sacral hiatus [23, 24]. Through this access corridor, the spinal canal can be directly and safely entered through no more than a 2-3mm incision and without the need for muscle or bony removal. This endoscopic technique, joined with laser-fiber-coupled delivery of LF-ablating laser technology, stands to provide a means by which the compressive pathology could be selectively removed. Work on uniting these technologies is ongoing.

Acknowledgments: We thank the MIT Lincoln Laboratory Advanced Concepts Committee and New Technology Initiatives Board for their support of this work. Also: Andrew Siegel, Emily Fenn, Christopher Ward, Fran Nargi, Peter Boettcher, Catherine Cabrera, Darren Rand, Seth Trotz, and Chuck Vanderburg. This work is sponsored by the Department of the Air Force under Air Force Contract #FA8721-05-C-0002. Opinions, interpretations, conclusions and recommendations are those of the author and are not necessarily endorsed by the United States Government.

References:

[1] Mekhail N, Costandi S, Abraham B, Wadie SS. Functional and patient-reported outcomes in symptomatic lumbar spinal stenosis following percutaneous decompression. Pain Practice July 2012; 12(6):417-25.

[2] Katz JN, Harris MB. Lumbar spinal stenosis. N Engl J Med 2008; 358:818–825.

[3] Schönström N, Lindahl S, Willén J, Hansson T. Dynamic changes in the dimensions of the lumbar spinal canal: an experimental study in vitro. J Orthop Res. 1989; 7:115–121.

[4] Hansson T, Suzuki N, Hebelka H, Gaulitz A. The narrowing of the lumbar spinal canal during MRI: the effects of the disc and ligamentum flavum. Eur Spine J 2009; 18:679–686.

[5] National Neurosurgical Procedural Statistics. American Association of Neurologic Surgeons 2006 .

[6] BeamGage User Guide, Document No: 50220-001, v6.6, 2015 May 8; 129.

[7] P. Mainil-Varlet, MD, PhD, D. Monin, MD, C. Weiler, MD, S. Grogan, PhD, T. Schaffner, MD, B. Züger, MSc, and M. Frenz, PhD. Quantification of Laser-Induced Cartilage Injury by Confocal Microscopy in an ex Vivo Model. The Journal of Bone & Joint Surgery April 2001; 83(4):566-566.

[8] Steketee, J. Spectral Emissivity of Skin and Pericardium. Phys Med Biol 1973; 18(5):686-694.

[9] Fried, N, New Technologies in Endourology: Potential Applications of the Erbium:YAG Laser in Endourology, Journal of Endourology, V. 15, Num. 9, Nov 2001, pp 889 – 894.

[10] Kalichman L, Cole R, Kim DH, Li L, Suri P, Guermazi A, Hunter DJ et al. Spinal stenosis prevalence and association with symptoms: the Framingham Study. Spine J July 2009; 9:545–550.

[11] Brouwer PA, Brand R, van den Akker-van Marle ME, Jacobs WC, Schenk B, van den Berg-Huijsmans AA, Koes BW, van Buchem MA, Arts MP, Peul WC. Percutaneous laser disc decompression versus conventional microdiscectomy in sciatica: a randomized controlled trial. Spine J May 2015; 15(5):857-865.

[12] Ren L, Han Z, Zhang J, Zhang T, Yin J, Liang X, Guo H, Zeng Y. Efficacy of percutaneous laser disc decompression on lumbar spinal stenosis. Lasers Med Sci May 2014; 29(3):921-923.

[13] Sato M, Ishihara M, Kikuchi M, Mochida J. The influence of Ho:YAG laser irradiation on intervertebral disc cells. Lasers Surg Med Nov 2011; 43(9):921-926.

[14] Lee DY, Lee SH. Carbon dioxide (CO2) laser-assisted microdiscectomy for extraforaminal lumbar disc herniation at the L5-S1 level. Photomed Laser Surg Aug 2011; 29(8):531-535.

[15] Gottlob C, Kopchok GE, Peng SK. Holmium:YAG Laser Ablation of Human Intervertebral Disc: Preliminary Evaluation. Lasers in Sugery and Medicine 1992; 12:86-91.

[16] Molex/Polymicro Technologies LLC, Phoenix: Brochure about Deep UV Enhanced Fibers (FDP).

[17] Venugopalan, V. Pulsed Laser Ablation of Tissue: Surface Vaporization or Thermal Explosion? SPIE Conf 2391, Laser-Tissue Interaction VI, 184. 1995; doi:10.1117/12.209881.

[18] Vogel A, Venugopalan V. Mechanisms of Pulsed Laser Ablation of Biological Tissues. Chem Rev 2003; 103:577-644.

[19] Viejo-Fuertes D, Liguoro D, Rivel J, Midy D, Guerin J. Morphologic and histologic study of the ligamentum flavum in the thoraco-lumbar region. Surg Radiol Anat 1998; 20:171-176.

[20] van Leeuwen TG, van Erven L, Meertens JH, Motamedi M, Post M, Borst C. Origin of arterial wall dissections induced by pulsed excimer and mid-infrared laser ablation in the pig. J Am Coll Cardiol 1992; 19(7):1610-1618.

[21] Kosaka H, Sairyo K, Biyani A, Leaman D, Yeasting R, Higashino K, Sakai T, Katoh S, Sano T, Goel VK, Yasui N. Pathomechanism of loss of elasticity and hypertrophy of lumbar ligamentum flavum in elderly patients with lumbar spinal canal stenosis. Spine (Phila Pa 1976) Dec 2007; 32(25):2805-11.

[22] Schräder PK, Grob D, Rahn BA, Cordey J, Dvorak J. Histology of the ligamentum flavum in patients with degenerative lumbar spinal stenosis. Eur Spine J 1999; 8(4):323-8.

[23] Purdy PD, Fujimoto T, Replogle RE, Giles BP, Fujimoto H, Miller SL. Percutaneous intraspinal navigation for access to the subarachnoid space: use of another natural conduit for neurosurgical procedures. Neurosurg Focus Jul 2005; 19(1):1-5.

[24] Fujimoto T, Giles BP, Replogle RE, Fujimoto H, Miller SL, Purdy PD. Visualization of sacral nerve roots via percutaneous intraspinal navigation (PIN) AJNR Am J Neuroradiol Oct 2005; 26(9):2420-4.